Synthesis, Biological Evaluation, and Pharmacophore Generation of Uracil, 4(3*H*)-Pyrimidinone, and Uridine Derivatives as Potent and Selective Inhibitors of Parainfluenza 1 (Sendai) Virus

Raffaele Saladino,*[,†] Claudia Crestini,[†] Anna Teresa Palamara,[‡,§] Maria Chiara Danti,[||] Fabrizio Manetti,[||] Federico Corelli,[||] E. Garaci,[§] and Maurizio Botta*[,||]

Dipartimento Agrochimico Agrobiologico, Università degli Studi di Viterbo "La Tuscia", via San Camillo de Lellis, 01100 Viterbo, Italy, Dipartimento di Biologia e Patologia Cellulare e Molecolare L. Califano, Università di Napoli Federico II, via Pansini 5, 80131 Napoli, Italy, Dipartimento di Medicina Sperimentale e Scienze Biochimiche, Università di Roma "Tor Vergata", via Tor Vergata 135, 00133 Roma, Italy, and Dipartimento Farmaco Chimico Tecnologico, Università degli Studi di Siena, via Aldo Moro, 53100 Siena, Italy

Received May 29, 2001

Several new 6-oxiranyl-, 6-oxiranylmethyluracils, and pyrimidinone derivatives, synthesized by lithiation−alkylation sequence of 1,3,6-trimethyluracil, 1,3-dimethyl-6-chloromethyluracil, and 2-alkoxy-6-methyl-4(3*H*)-pyrimidinones, showed a potent and selective antiviral activity against Sendai virus (SV) replication. To gain insight into the structural features required for SV inhibition activity, the new compounds were submitted to a pharmacophore generation procedure using the program Catalyst. The resulting pharmacophore model showed high correlation and predictive power. It also rationalized the relationships between structural properties and biological data of these inhibitors of SV replication.

Introduction

Sendai virus (SV) is a murine subtype of parainfluenza 1 viruses (PIVs) belonging to the family of *Paramyxoviridae*. SV is an enveloped virus with nonsegmented negative strand RNA and six major structural proteins. Nucleoprotein (NP), large (L) protein, and P protein are associated with the nucleocapside, while hemagglutinin-neuraminidase (HN), fusion (F), and matrix (M) proteins constitute the envelope. The surface glycoproteins F and HN are the most important viral antigens that induce humoral immune response in the hosts.[1]

PIV types 1, 2, and 3 were first discovered in 1956[2] and were recognized as important human pathogens causing upper and lower respiratory tract infections. In particular, they were identified as the major causes of croup or laryngotracheobronchitis in children.[3,4]

In older children and adults PIVs cause frequent reinfections that are generally mild in healthy persons but may cause serious outcomes in immunocompromized patients or patients with underlying cardiopulmonary diseases.[5,6] Immunocompromized hosts often have upper respiratory tract symptoms similar to those experienced by normal hosts, as well as a higher incidence of lower respiratory tract symptoms. Lower respiratory tract infection can lead to respiratory failure and death in bone marrow transplantation recipients of all ages, especially if the infection occurs in the period soon after transplantation.[7,8]

To date, there is no licensed antiviral therapy for the treatment of PIV infections. Ribavirin, a broad-spectrum antiviral agent, is effective against PIV in cell culture and has been used for the treatment of lower respiratory tract disease in immunocompromized hosts.[9] Case reports documenting decreased viral load and clinical improvement in children with severe combined immunodeficiency following multiple treatments with aerosolized ribavirin therapy have been described.[10] However, the efficacy of therapy with ribavirin is still under debate[11] and the potential environmental release of drug has caused concern in hospital personnel because of the potential teratogenicity in the rodent model.[12]

At present, there is a lack of effective monotherapies for specific respiratory viruses, particularly for parainfluenza viruses.

Sendai virus has been extensively used in studies that have defined many of the basic biochemical and molecular biological properties of the paramyxoviruses. Moreover, it has been employed as an in vivo experimental model of parainfluenza virus infection or for in vitro studies of new antiviral agents.[13]

Even if low molecular weight compounds such as thapsigargin (a specific inhibitor of Ca^{2+}-ATPase),[14] ambazone (1,4-benzoquinone-guanylhydrazone-thiosemicarbazone),[15] dihydroheptaprenol,[16] and methylprednisolone acetate[17] have been tested, selective and specific antiviral agents against SV have been reported for the first time by our research group.[18]

In particular, some 6-(oxiranylmethyl)uracil derivatives (compounds **2a**−**g** in Scheme 1), prepared during a general screening of anti-HIV compounds, showed very interesting activity as inhibitors of Sendai virus even if associated with a non-negligible toxicity (evaluated as alteration of normal cell morphology, viability, and count).[18]

The goal of this work was the synthesis of new uracil, pyrimidinone, and uridine derivatives possibly characterized by high affinity and selectivity toward SV. In

* To whom correspondence should be addressed. For R.S.: phone, +39 0761 357284; fax, +39 0761 354272; e-mail: saladino@unitus.it. For M.B.: phone, +39 0577 234306; fax, +39 0577 234333; e-mail: botta@unisi.it.
† Università degli Studi di Viterbo "La Tuscia".
‡ Università di Napoli Federico II.
§ Università di Roma "Tor Vergata".
|| Università degli Studi di Siena.

10.1021/jm010938i CCC: $20.00 © 2001 American Chemical Society
Published on Web 11/22/2001

Scheme 1

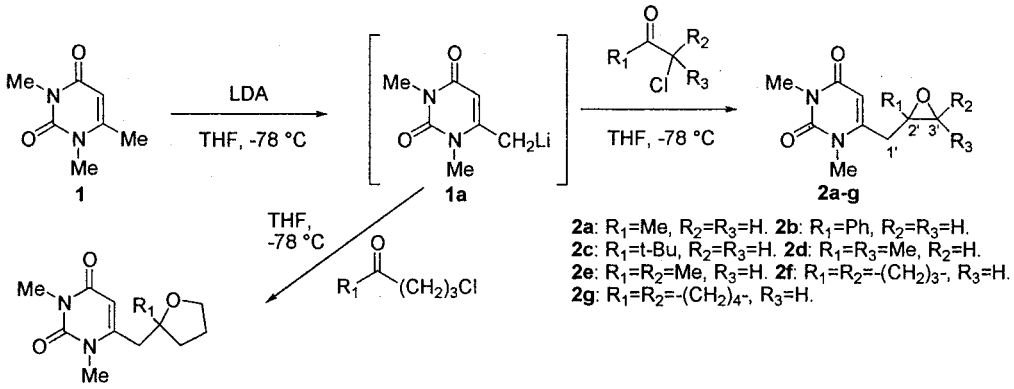

Table 1. Measured and Calculated Activity against Parainfluenza 1 (Sendai) Virus and Cytotoxicity of the New Compounds

compd	measured ED_{50},[a] μM	calculated ED_{50}, μM	stereochemistry assigned by the program[b]	MTC,[c] μM	CC_{50},[d] μM
2a	0.24	0.82	*R*	0.48	4.0
2b	0.18	0.13	*S*	0.37	3.7
2c	0.59	0.57	*S*	>0.79	7.9
2d[e]	>2	2.2	*S,R*[f]	>2	89
2e[e]	>2	3	*S,S*[f]	>2	89
2f	0.42	0.97	*R,R*[f]	>0.84	8.4
2g[e]	>2	0.72	*S,S*[f]	>2	40
3a[e]	338	320	S	446	1218
3b	1.11	0.75	*S*	>223	1380
3c	116	60	*S*	>333	547
5a	176	170	*R,R*[f]	>352	>352
5b	16.6	24	*S*	330	>330
5c	147	42	*S*	294	>294
5d	171	320	*R,S*[f]	342	>342
5e	0.37	14 (4.4)[h]	*S*	735	>360
6a	166	76	*S*	383	130
6b	152	130	*S*	305	170
6c[e]	146	110	*S*	292	90
6d	893	6.9	*S*	893	1620
6e	187	220	*S*	>376	860
6f[e]	164	220	*S*	326	816
6g	186	230	*S*	373	1082
6h[e]	>446	300	*S*	446	1218
6i	300	290	*S*	397	1016
6j	195	110	*S*	376	579
8	267	270	*S*	>305	375
10a	0.47	1	*R,R*[g]	>0.81	7.3
10b	0.38	0.57	*R,S*[g]	>0.80	7.7
10c	193	160	*R,R*[g]	380	>380

[a] Inhibitory concentration required to reduce virus yield by 50%. [b] Assigned to each compound by the program with the aim of fitting the pharmacophore model (see Experimental Section). [c] Minimun toxic concentration required to cause a microscopically detectable alteration of normal cell morphology. The results listed are the mean values of two or three independent determinations. [d] Concentration required to inhibit cell proliferation by 50%. [e] Compounds constituting the test set. [f] Refers to the chiral center at the 2′- and 3′-positions, respectively. [g] Refers to the chiral center at the 1′- and 2′-positions, respectively. [h] In parentheses is the calculated activity for an alternative orientation of **5e** in the pharmacophore model (see text).

this paper we report the synthesis and biological evaluation of compounds **3a**−**c, 5e**, **6a**−**j**, **8** (Schemes 1−3 and Table 1), and **12a,b** and **13**−**15** (Scheme 5) showing good anti-SV activity associated with very low toxicity. We also provide a full description of the synthetic preparation and biological evaluation of compounds **2a**−**g**, **5a**−**d**, and **10a**−**c**.

In addition, to investigate the structure−activity relationships of these compounds, we have applied the program Catalyst[19] to develop a pharmacophore model for SV inhibitors. The calculated model, able to rationalize the relationships between the chemical features of the new structures and their biological data, consists of a hydrophobic region and three hydrogen bond acceptor features. It shows a good statistical significance (r = 0.85, rmsd = 1.40) and successfully predicts the affinities of the molecules of, and external to, the training set.

Chemistry

Apart from 1-[(2-hydroxyethoxy)methyl]-6-(phenylthio)thymine (HEPT) and 3,4-dihydro-2-alkoxy-6-benzyl-4-oxypyrimidine (DABO) derivatives,[20] only little scattered data are available concerning the antiviral activity of 6-substituted pyrimidines and uracils probably because the preparation of such compounds is not a trivial task.[21]

Our previous work on the synthesis of bipyrimidinones and bipyrimidinylmethane derivatives showed that the metalation of 6-methyl-4(3*H*)-pyrimidinones takes place at the methyl in the 6-position in an essentially regiospecific manner.[22] This metalation−alkylation sequence was used for the preparation of several types of 6-substituted uracils.[23]

To fully exploit the synthetic potential of this procedure, we started to investigate the reaction of the lithium derivative of 1,3,6-trimethyluracil **1** with several acyclic and cyclic α-halogenoketones as electrophiles. The reaction of **1a**, prepared from **1** with lithium diisopropylamide (LDA, 1.2 equiv) in THF at −78 °C, with chloroacetone, 2-chloroacetophenone, 1-chloropinacolone, 3-chloro-2-butanone, 2-chlorocyclopentanone, and 2-chlorocyclohexanone, afforded 6-oxiranylmethyl uracil derivatives **2a**−**g** (Scheme 1) in acceptable yields (Table 2).

In the case of 3-chloro-2-butanone, two possible diastereoisomers, compounds **2d** and **2e**, were obtained after chromatographic purification (ratio value **2d**/**2e** = 1:5), and their stereochemistry was determined by a series of 1D-NMR nuclear Overhauser effect (NOE) measurements. In particular, the proximity of the 2′-Me and 3′-Me protons in **2e** was revealed by their mutual NOE effect (8.1%), suggesting the *E* stereochemistry. On the other hand, the *Z* stereochemistry of

Scheme 2

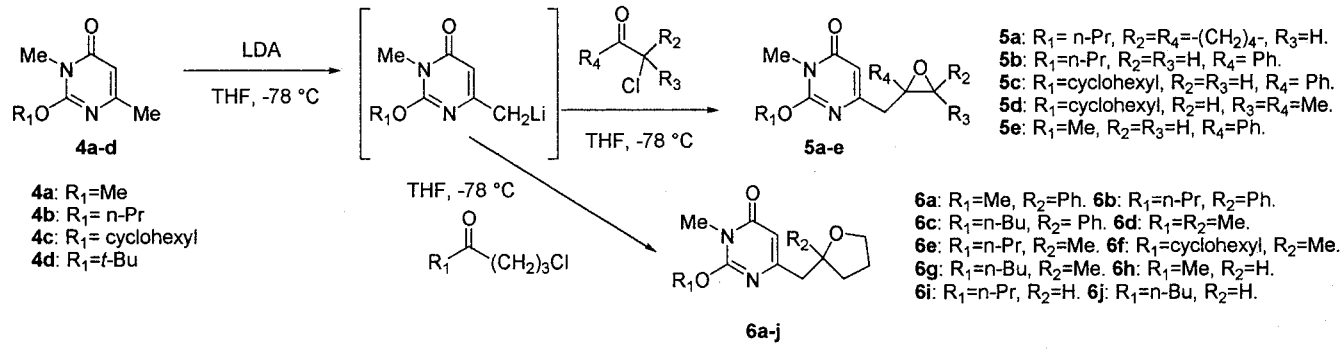

Table 2. Chemical and Physical Data of the New Compounds

compd	formula	mp, °C	yield, %
2a	$C_{10}H_{14}N_2O_3$	oil	48
2b	$C_{17}H_{18}N_2O_3$	oil	65
2c	$C_{13}H_{20}N_2O_3$	85.8	67
2d	$C_{11}H_{16}N_2O_3$	oil	20
2e	$C_{11}H_{16}N_2O_3$	oil	47
2f	$C_{12}H_{16}N_2O_3$	oil	68
2g	$C_{13}H_{18}N_2O_3$	155−157	83
3a	$C_{11}H_{16}N_2O_3$	73−75	21
3b	$C_{12}H_{18}N_2O_3$	82−84	23
3c	$C_{17}H_{20}N_2O_3$	oil	18
5a	$C_{15}H_{22}N_2O_3$	oil	40
5b	$C_{17}H_{20}N_2O_3$	oil	65
5c	$C_{20}H_{24}N_2O_3$	oil	69
5d	$C_{16}H_{24}N_2O_3$	oil	73
5e	$C_{15}H_{16}N_2O_3$	oil	81
6a	$C_{17}H_{20}N_2O_3$	oil	15
6b	$C_{20}H_{26}N_2O_3$	oil	36
6c	$C_{20}H_{26}N_2O_3$	oil	63
6d	$C_{13}H_{20}N_2O_3$	oil	85
6e	$C_{14}H_{22}N_2O_3$	oil	35
6f	$C_{17}H_{26}N_2O_3$	oil	41
6g	$C_{15}H_{24}N_2O_3$	oil	46
6h	$C_{11}H_{16}N_2O_3$	oil	33
6i	$C_{13}H_{20}N_2O_3$	oil	23
6j	$C_{14}H_{22}N_2O_3$	oil	38
8	$C_{14}H_{22}N_2O_3$	oil	78
10a	$C_{14}H_{16}N_2O_3$	oil	56
10b	$C_{14}H_{14}N_2O_3$	129−131	43
10c	$C_{14}H_{14}N_2O_3$	162	35
12a	$C_{35}H_{32}N_2O_3$	oil	80
12b	$C_{40}H_{34}N_2O_3$	oil	69
13	$C_{37}H_{36}N_2O_{10}$	oil	47
14	$C_{37}H_{36}N_2O_{10}$	oil	28
15	$C_{42}H_{42}N_2O_{10}$	oil	23

2d was confirmed by the lack of any detectable NOE effect between 2′-Me and 3′-Me protons.

In a similar way, starting from **1**, by application of the same metalation reaction described above, followed by quenching with 4-chlorobutyraldehyde,[24] 5-chloro-2-pentanone, and 1-phenyl-4-chloro-1-butanone, the 1,3-dimethyl-6-(tetrahydrofuranylmethyl)uracils **3a**−**c** (Scheme 1) were obtained in yields ranging between 18% and 23% (Table 2).

The same metalation−alkylation sequence performed on 2-alkyloxy-3,6-dimethyl-4(3*H*)-pyrimidinones **4a**−**d**, using various electrophiles, afforded compounds **5a**−**e** and **6a**−**j** (Scheme 2). It is interesting to note that the possible formation of bipyrimidinylmethane derivates or C-2 transalkoxylation reactions (see below for the preparation of compounds **4b**−**d**) were not operative side processes under these experimental conditions. In particular, by using 2-methoxy-, 2-*n*-propyloxy-, and 2-cyclohexyloxy-3,6-dimethyl-4(3*H*)-pyrimidinones (**4a**, **4b**, and **4c**, respectively), in the presence of 2-chlorocyclohexanone, 2-chloroacetophenone, and 3-chloro-2-butanone, the reaction sequence afforded 6-oxiranylmethyl-4(3*H*)-pyrimidinone derivatives **5a**−**e** (Scheme 2) in yields ranging from 40% to 81% (Table 2). The proximity of the 2′-Me and 3′-H protons of **5d** was revealed by their mutual NOE effect (9%), leading to the conclusion that this compound represents the *Z* isomer.

Scheme 3

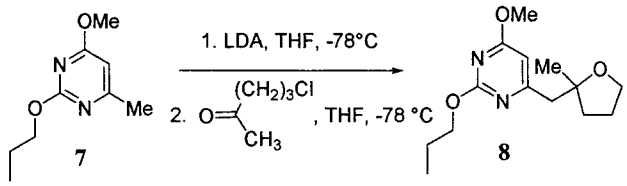

Compound **4a** was prepared by regiospecific N-3 methylation of 2-methoxy-6-methyl-4(3*H*)-pyrimidinone with dimethyl sulfate (Me_2SO_4) in NaOH (30% aqueous solution) at room temperature in 90% yield. **4b**−**d** were prepared by the transalkoxylation reaction of the same substrate with appropriate sodium alkoxides,[25] followed by methylation of the new obtained 2-alkoxy derivatives. In the latter case, the alkylation of 2-*n*-propyloxy-6-methyl-4(3*H*)-pirimidinone with Me_2SO_4 in NaOH (30% aqueous solution) at 25 °C gave the desired N-3 derivative **4b** as the only recovered product. The same reaction performed with CH_2N_2 in MeOH at 25 °C afforded both the N-3 methyl derivative **4b** and the O-4 methyl derivative **7**. Compound **7** was also used as starting material for the metalation−alkylation procedure to give compound **8** (Scheme 3).

With the aim of applying this procedure to the synthesis of 6-oxiranyluracil derivatives, we studied the reaction of the lithium derivative of 1,3-dimethyl-6-chloromethyluracil **9** with various carbonyl compounds as electrophiles. The reaction of **9a**, prepared from **9** with LDA (1.2 equiv) in THF at −78 °C with acetophenone and benzaldehyde afforded compounds **10a**−**c** (Scheme 4) in acceptable yields (Table 2). In compound **10a**, obtained as the only recovered product, the proximity of the 2′-Phe and 1′-H protons was revealed by their mutual NOE effects (7.5%), suggesting the *E* stereochemistry. In the case of diastereoisomers **10b** and **10c** (ratio value **10b**/**10c** = 1:1.2) the stereochemistry was assigned on the basis of the value of the coupling constant between vicinal 1′-H and 2′-H protons (8.3, and 1.9 Hz, respectively), suggesting the *Z* stereochemistry for **10b** and the *E* stereochemistry for **10c**.

Scheme 4

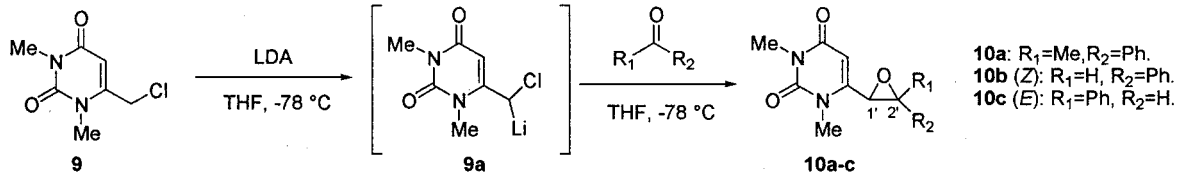

Scheme 5

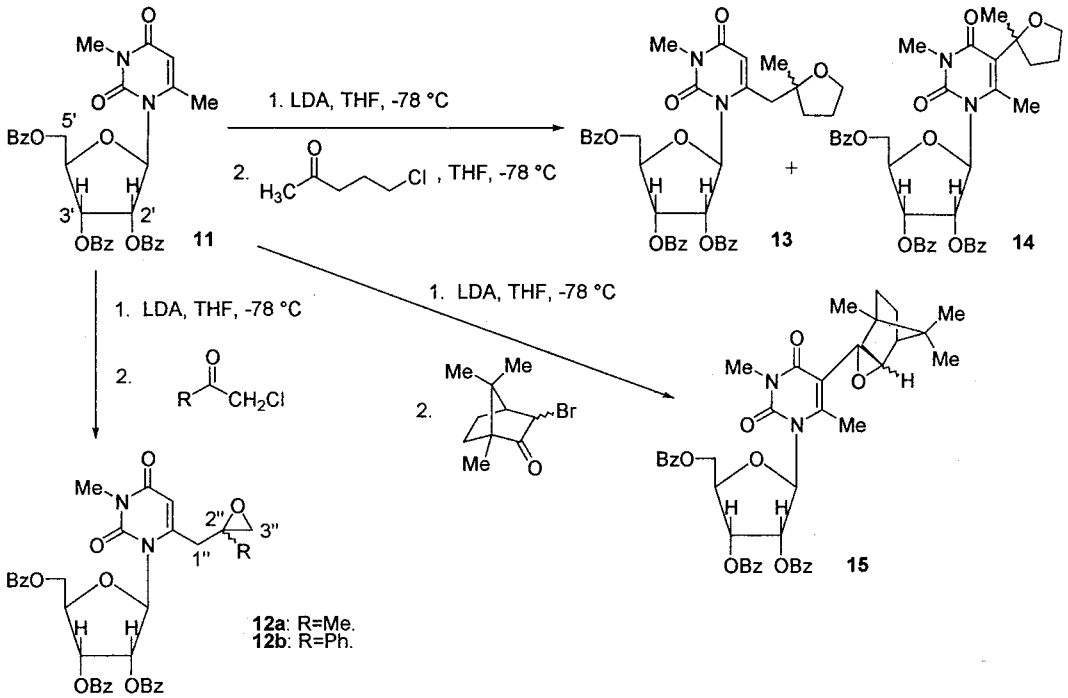

Finally, to evaluate the influence on the anti-SV activity of a sugar substituent at the N-1 of the uracil ring, 2′,3′,5′-tri-*O*-benzoyl-3,6-dimethyluridine **11**[26] was treated with chloroacetone and 2-chloroacetophenone in the presence of LDA in dry THF at −78 °C (Scheme 5). Under these experimental conditions the corresponding 6-(oxiranylmethyl)uridine derivatives **12a,b** were obtained as a chromatographically unseparable mixture of diastereoisomers (ratio value 1:1) in 80% and 69% yield, respectively (Table 2). Even if the synthesis of 5-oxiranyluridines is described in the literature,[27] to the best of our knowledge, this is the first report dealing with the preparation of uridine derivatives bearing the oxiranyl moiety in the C-6 position. The reaction was then performed, under similar experimental conditions, with 5-chloro-2-pentanone as the electrophile. The 6-(tetrahydrofuranylmethyl)uridine derivative **13** and the unexpected 5-(tetrahydrofuranyl)uridine derivative **14** (Scheme 5) were obtained in 47% and 28% yield, respectively. The structure of compound **14** was confirmed by the presence of an absorption signal of the C-6 methyl moiety in the ^{1}H NMR, while the integrity of the C5−C6 double bond was verified by its IR spectrum. We have not studied in detail the mechanism of this reaction, but it is reasonable to suggest that the N-1 sugar moiety in the syn orientation of the nucleoside may affect the access of a very sterically demanding electrophile, such as 5-chloro-2-pentanone, to the 6-position. Thus, the C-5 alkylation may occur, through a mesomeric form, as a side reaction. This hypothesis is further confirmed by a probe experiment where an ever more sterically hindered α-halogenoketone, the racemic 3-bromocamphor, was used as an electrophile. In this case, the corresponding C5-alkylated uridine derivative **15** was obtained as the only recovered product in low yield (23%) besides the unreacted substrate.

Bioassay Results

All new products have been evaluated for their antiviral activity against parainfluenza 1 replication in Madin Darby canine kidney cells (MDCK cells).

To test viral production, supernatants from infected cells (see Experimental Section) were harvested at different time points after virus challenge and were tested by measuring the hemagglutinin units (HAU), as described by Garaci.[28] In confluent MDCK cells, cytotoxicity was evaluated on the basis of microscopic examination of cell morphology, evaluation of cell viability after tripan blue staining, and cell count. The viability of proliferating mouse myeloma cells (NSO cells from American Tissue Culture Collection) and normal human lymphocytes stimulated with PHA (5 μg/mL) was measured by using tritiated thymidine incorporation tests. Statistical evaluation of the results allowed us to calculate CC_{50} for both proliferating mouse myeloma cells and normal human lymphocytes.

Most of the analyzed compounds showed interesting inhibitory activity. In particular, **2a**−**c**, **2f**, **5e**, and **10a**,**b** presented an ED_{50} (the inhibitory concentration required to reduce virus yield by 50%) lower than micromolar, while most of the remaining compounds

were about 3 orders of magnitude less potent (Table 1). Moreover, **3b** presented a micromolar ED_{50} (1.1 μM) with a selectivity index of about 200.

Some of the tested compounds showed an associated toxic effect that, in the case of **2c**, **2f**, **3b**−**d**, **5a**, **6e**, and **8**, was not microscopically detectable at the concentration range in which compounds have been found active.

Results and Discussion

On the basis of the biological results reported above, the following structure−activity relationships can be tentatively reported. (i) The *N*,*N*-dimethyluracil scaffold, very unusual for antiviral compounds, along with the 6-substitution on the uracil ring, seems to be an important feature for active compounds. (ii) The substitution pattern and the stereochemistry of the oxirane ring play an important role in modulating both the activity and the toxic effect of the products. In particular, the 6-oxiranyl derivatives **10a** and **10b**, and the 6-oxiranylmethyl derivatives **2a**−**c**, **2f**, and **5e** showed very interesting activity depending on the size of the hydrophobic substituent at the 2′-positions, with the phenyl moiety associated with the best activity values (**2b**, **5e**, **10a**,**b**). Moreover, the influence of the stereochemistry on the antiviral activity can be highlighted in **10b**,**c**, with the former about 3 orders of magnitude more active. (iii) The substitution of the oxiranyl moiety with a tetrahydrofuranyl ring resulted in less active compounds, with the exception of **3b**, which is only 1 order of magnitude less active with respect to **2b**. Compound **3b** showed an interesting selectivity index (about 200) as a consequence of decreased toxic effects. In addition, substituents at the 2′-position on the tetrahydrofuranyl ring play an important role in modulating both the activity and the toxic effect. In fact, derivatives bearing a phenyl ring at the 2′-position showed the highest activities, with **6c** being the most active compound of this series. The presence of a methyl group at the same position gave rise to less active products associated with low (**6e**) or no (**6d**) toxicity. Unsubstituted derivatives are characterized by low values of inhibitory activity and relevant toxicity. (iv) Finally, nucleosides **12** and **13** showed an appreciable antiviral activity.[29]

From the biological data reported in Table 1, it can be seen that most of the cytotoxicity values associated with the compounds are comparable to the values of the antiviral activity. In fact, anti-SV activity for each compound is very similar to the MTC and CC_{50} values. Few exceptions to this trend are worthy of consideration. In particular, compound **5b** is characterized by a cytotoxic concentration about 20-fold higher than the antiviral dose (330 vs 16.6 μM, respectively). Moreover, compound **5e** shows a very interesting biological profile with cytotoxic concentration at least 3 orders of magnitude higher than the antiviral dose (>360 vs 0.37 μM, respectively). Finally, **3b** is characterized by a selectivity index of about 200, with an antiviral activity 1 order of magnitude higher than the most active compound **2b**.

Computational Studies. To obtain a better understanding of the SARs of the above-described inhibitors of Sendai virus replication, we performed molecular modeling and pharmacophore generation experiments using Catalyst software.

In particular, we report a study that applies a ligand-based drug design (pharmacophore development) method to rationalize the relationships between structures and biological data. Accordingly, experimentally determined affinities are used to derive a pharmacophore model that describes the three-dimensional structural properties required to have profitable interactions with the corresponding binding site on SV.

This computational approach has been applied to a set of 22 Sendai virus inhibitors (the training set, Table 1) chosen according to the Catalyst guidelines.[30] These compounds are characterized by activity values spanning ~3.7 orders of magnitude, the minimum value of 0.18 μM being associated with compound **2b** and the maximum value of 893 μM being associated with compound **6d**.

Because no experimental data on the biologically relevant conformations of the selected compounds (for example, atomic coordinates derived from X-ray crystallographic studies of their complexes with the putative receptor) are available, we resorted to a molecular mechanics approach to build the conformational model to be used for pharmacophore generation. The molecules were built within Catalyst and submitted to conformational analysis. All the conformers of each compound, within a range of 20 kcal/mol with respect to the global minimum, have been employed to derive a set of pharmacophore hypotheses.

The resulting pharmacophore hypotheses use chemical functions and their spatial location to explain the differences in inhibitory activity within the training set. The measured and calculated activity values for both the training set and the test set are listed in Table 1. All but 1 of the 10 generated hypotheses have in common the presence of three hydrogen bond acceptor groups (HBA) and one hydrophobic region (HY). Only one selected hypothesis possesses an additional hydrophobe as a common chemical function instead of a hydrogen bond acceptor.

Hypothesis 1, characterized by the highest scoring and the best statistical parameters (correlation coefficient and root-mean-square deviation (rmsd)), is the most likely to yield relevant information about the pharmacophore elements of the studied compounds. Accordingly, hypothesis 1 has been chosen to represent "the pharmacophore model".

The regression analysis of "true" versus "estimated" SV inhibition activity values for the training set exhibited a correlation coefficient r of 0.85 and an rmsd of 1.40. Moreover, because of the relatively small range of bits between hypothesis 1 and the null hypothesis (45 bits) corresponding to about a 75% chance of true correlation, special care was taken to evaluate the statistical significance of the pharmacophore model. In particular, a randomized trial procedure derived from the Fischer method[31] was applied to the training set. Experimental activities were scrambled 19 times to obtain spreadsheets with randomized data. Nineteen pharmacophore generation runs were performed using the scrambled training sets. As a result, among the 190 resulting pharmacophore hypotheses, none was found with a lower cost than hypothesis 1, suggesting that there was at least a 95% chance of true correlation in

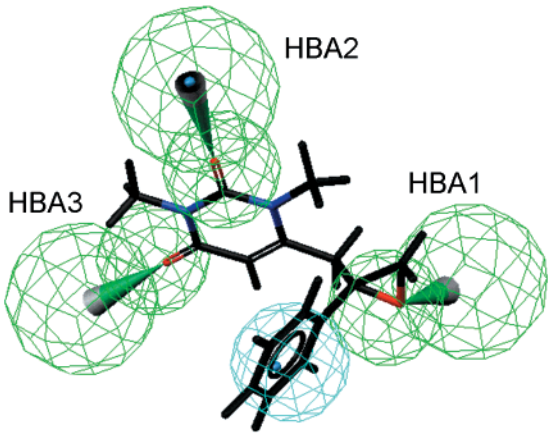

Figure 1. Compound **2b** mapped to the four-feature best hypothesis (the pharmacophore model) for Sendai virus inhibitors. Chemical functionalities are color-coded: blue for a hydrophobic region (HY) and green for hydrogen bond acceptors (HBA1, HBA2, and HBA3).

the biological data. These findings indicate a reliable ability to estimate the affinities of the training set.

As a representative example, Figure 1 shows the best-fitted conformer of **2b** (the most active compound of the training set) into the pharmacophore model characterized by three hydrogen bond acceptors and a hydrophobic feature. The chemical functionalities of this hypothesis are matched by the chemical groups of **2b**. The phenyl ring fits within the region of the hydrophobic group (HY), the carbonyl groups at the 2- and 4-position occupy two hydrogen bond regions (HBA2 and HBA3, respectively), and finally, the oxirane oxygen is located in the third hydrogen bond acceptor region (HBA1) of the hypothesis. The conformer shown has a calculated energy of 1.1 kcal/mol above the calculated lowest energy conformer of compound **2b**, and its activity is properly estimated by the pharmacophore hypothesis (estimated activity of 0.13 μM versus an experimental value of 0.18 μM).

Compounds **2a**, **2c**, and **2f** showed very similar orientation with the respect to **2b**, the methyl, *tert*-butyl, and a portion of the condensed cyclohexyl substituent at the 2′-position, respectively, lying within the hydrophobic region of the hypothesis.

The pharmacophore hypothesis is also able to distinguish between **10b** (*Z* stereochemistry, $ED_{50} = 0.38$ μM) and **10c** (*E* stereochemistry, $ED_{50} = 193$ μM). Figure 2 shows the mapping of these two isomers on hypothesis 1. While compound **10b** shows the same alignment on the hypothesis as compound **2b**, the phenyl ring of compound **10c** cannot interact with the hydrophobic region, resulting in a lower estimated activity (the activities of compounds **10b** and **10c** were correctly estimated in 0.57 and 160 μM, respectively).

Compounds **5a**−**e** of the training set are characterized by structural properties similar to those of compounds **2a**−**g** and, as expected, present similar orientations. The key difference in the alignment of compounds **2** and **5** to the pharmacophore hypothesis is the consequence of the alkoxy substitution at the 2′-position. In fact, compounds **5** cannot reach one (the hydrogen bond acceptor site HBA2) of the functional regions of the hypothesis, resulting in a lower estimated activity. Moreover, compounds **5b** and **5c** are predicted to be

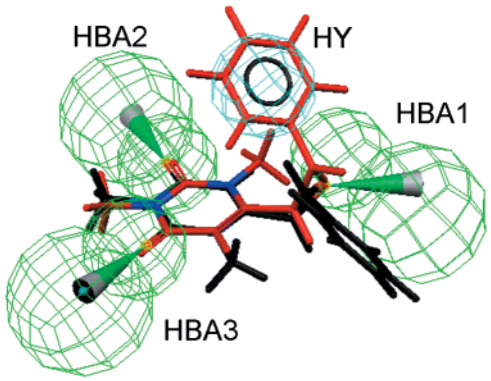

Figure 2. Compound **10b** (*Z* enantiomer, in red) and **10c** (*E* enantiomer, in black) mapped to the four-feature best hypothesis (the pharmacophore model) for Sendai virus inhibitors. The aromatic ring of **10c** cannot reach the hydrophobic region (HY, blue) of the hypothesis. Color codes are as in Figure 1.

more active than **5a** and **5d** (24 and 42 μM versus 170 and 320 μM, respectively) because of their phenyl group that can function as a hydrophobic moiety fulfilling the hydrophobic site HY of the hypothesis. On the other hand, the methyl substituent at the 2′-position and the condensed cyclohexyl ring of compounds **5a** and **5d**, respectively, match HY less well than **5b** or **5c**. These considerations suggest that the mapping to the hydrophobic feature of the hypothesis could explain the order of magnitude difference in measured activity for compounds **5b** and **5c** with respect to **5a** and **5d**.

Finally, the proposed model is unable to distinguish between compounds **5b** and **5c** probably because the hydrophobic group at the 2′-position, representing the sole structural difference between the two compounds (cyclohexyl versus *n*-propyl, respectively), lies in a region of space defined by a hydrogen bond acceptor site.

Compounds **5e** and **5b** have the same alignment on the hypothesis as **2b**, and their lower estimated activity (14 and 24 μM, respectively) is explained by a missing hydrogen bond acceptor group interacting with HBA2. There is also an alternative mapping for **5e** (estimated activity 4.4 μM) that places the alkoxy oxygen atom much closer to the center of the HBA function, resulting in the proper interaction with the feature itself. These findings led to the suggestion that the lack of interaction involving the HBA feature at the 2′-position of the inhibitors seems to be important for rationalizing the trend of the activity values associated with compounds **2b**, **5e**, **5b**, and **5c**. In addition, the substituent at the 2′-position, which can allow for interaction with the HBA feature of the hypothesis, is also the structural key element in the case of the subset consisting of **3b**, **6d**, **6e**, **6f**, and **6g**. While compounds **3b** and **6d**, which are able to make contact with the HBA2 feature, show an estimated activity of 0.75 and 6.9 μM, the activities of **6e**−**g** are predicted to be about 2 orders of magnitude less (220, 220, and 230 μM, respectively), in good agreement with experimental data. Moreover, the additional lack of activity associated with compounds **3a**, **6h**, **6i**, and **6j** could be attributed to the susbstitution of the 2′-methyl group with a hydrogen atom and consequent decreased fitting of superimposition onto the HY pharmacophore feature.

In light of these considerations, the HBA2 described above could play a very important role in defining the

activity for all the compounds of the training set. In fact, it is remarkable that the check performed by the program for surface accessibility of the molecular features[32] (see Experimental Section) has found that all the weakly active molecules are lacking a chemical moiety that could function as a hydrogen bond acceptor group corresponding to HBA2.

Conclusions

A qualitative structure−activity relationship analysis suggested that the *N*,*N*-dimethyluracil scaffold associated with a 2- and/or 6-substitution seems to show an important role in determining the activity against SV. On the other hand, substituents at both the N-1 and C-5 positions are still suitable in the search for more active and less toxic SV inhibitors.

More accurate and quantitative SAR considerations have been made by means of a pharmacophore model for SV inhibitors. This computationally built model is able to account for the major SARs associated with the new compounds, mainly on the basis of a pharmacophore hydrophobic region and a hydrogen bond acceptor group. In fact, both these features are common structural elements of compounds characterized by high activity toward the Sendai virus.

Experimental Section

Chemistry. NMR spectra were recorded on a Bruker (200 MHz) spectrometer and are reported in δ values. Mass spectra were recorded on a VG 70/250S spectrometer with an electron beam of 70 eV. Elemental analyses were performed by a Carlo Erba 1106 analyzer. Infrared spectra were recorded on a Perkin-Elmer 298 spectrophotometer using NaCl plates. All solvents are ACS reagent grade and were redistilled and dried according to standard procedures. Melting points were recorded on a Mettler FP-80 apparatus. Chromatographic purifications were performed on columns packed with Merck silica gel 60, 230−400 mesh for the flash technique. Thin-layer chromatography was carried out using Merck platten Kieselgel 60 F254.

General Procedure for the Synthesis of Compounds 2a−g and 5a−e. An Example: 1,3-Dimethyl-6-(2′-methyl-2′-oxiranylmethyl)uracil (2a). To a solution of compound **1** (1 mmol) in dry THF (6 mL) cooled to −78 °C, freshly prepared lithium diisopropylamide (LDA, 1.2 mmol) was added dropwise under nitrogen atmosphere. After the mixture was stirred for 30 min, chloroacetone (1.3 mmol) was added while maintaining the temperature below −70 °C. The mixture was stirred for 6 h, quenched with a saturated NH_4Cl solution (1 mL), and allowed to warm to room temperature. The organic layer diluted with EtOAc (60 mL) was then separated, dried with Na_2SO_4, and evaporated under reduced pressure. The residue was purified by flash chromatography using $CHCl_3$/MeOH = 9.5:0.5 as the mobile phase to give compound **2a** in 48% yield (Table 1): oil, ν_{max} (cm^{-1}) 1690, 1660, 1490, 1370; δ_H ($CDCl_3$) 1.34 (3H, s, CH_3), 2.75 (2H, dd, J = 14.44 Hz, CH_2), 3.21 (3H, s, *N*-CH_3), 3.43 (3H, s, *N*-CH_3), 3.49 (2H, dd, J = 14.44 Hz, CH_2), 5.62 (1H, s, C_5−H); δ_C ($CDCl_3$) 25.48 (CH_3), 27.92 (CH_3), 33.12 (CH_3), 40.00 (CH_2), 52.51 (CH_2), 72.41 (C), 102.94 (CH), 151.46 (C), 152.59 (C), 162.36 (C). Anal. ($C_{10}H_{14}N_2O_3$) C, H, N. MS: m/e = 210 (M^+).

General Procedure for the Synthesis of Compounds 3a−c, 6a−j, and 8. An Example: 1,3-Dimethyl-6-(2′-tetrahydrofurylmethyl)uracil (3a). To a solution of compound **4a** (1 mmol) in dry THF (6 mL) cooled to −78 °C, freshly prepared lithium diisopropylamide (LDA, 1.2 mmol) was added dropwise under a nitrogen atmosphere. After the mixture was stirred for 30 min, 5-chloro-2-pentanone (1.3 mmol) was added while maintaining the temperature below −70 °C. The mixture was stirred for 6 h, quenched with a saturated NH_4Cl solution (1 mL), and allowed to warm to room temperature. The organic layer diluted with EtOAc (60 mL) was then separated, dried with Na_2SO_4, and evaporated under reduced pressure. The residue was purified by flash chromatography using $CHCl_3$/MeOH = 9.5:0.5 as the mobile phase to give compound **3a** in 15% yield (Table 1): mp 73−75 °C (EtOAc/*n*-hexane), ν_{max} (cm^{-1}) 1690, 1665, 1520; δ_H ($CDCl_3$) 1.80 (2H, m, CH_2), 2.01 (2H, m, CH_2), 2.46 (2H, m, CH_2), 3.34 (3H, s, *N*-CH_3), 3.40 (3H, s, *N*-CH_3), 3.50 (2H, m, *O*-CH_2), 3.93 (1H, m, CH), 5.60 (1H, s, CH); δ_C ($CDCl_3$) 26.13 (CH_2), 27.78 (CH_3), 30.39 (CH_2), 33.31 (CH_2), 65.62 (CH), 68.12 (CH_2), 97.04 (CH), 153.81 (C), 161.94 (C), 170.0 (C). Anal. ($C_{11}H_{16}N_2O_3$) C, H, N. MS: m/e = 224 (M^+).

General Procedure for the Synthesis of Compounds 10a−c. An Example: (*E*)-1,3-Dimethyl-6-(2′-methyl-2′-phenyl-1′-oxiranyl)uracil (10a). To a solution of 1,3-dimethyl-6-chloromethyl uracil **9** in dry THF (6 mL) cooled to −78 °C, freshly prepared lithium diisopropylamide (LDA, 1.5 mmol) was added dropwise under a nitrogen atmosphere. After the mixture was stirred for 30 min, acetophenone (1.3 mmol) was added while maintaining the temperature below −70 °C. The mixture was stirred for 6 h, quenched with a saturated NH_4Cl solution (1 mL), and allowed to warm to room temperature. The organic layer diluted with EtOAc (60 mL) was then separated, dried with Na_2SO_4, and evaporated under reduced pressure. The residue was purified by flash chromatography using $CHCl_3$/MeOH = 9.5:0.5 as the mobile phase to give compound **10a** in 56% yield (Table 1): oil, ν_{max} (cm^{-1}) 1700, 1655; δ_H ($CDCl_3$) 1.86 (3H, s, CH_3), 3.17 (3H, s, *N*-CH_3), 3.37 (3H, s, *N*-CH_3), 3.86 (1H, s, CH), 5.69 (1H, s, CH), 7.24 (5H, m, Ph-H); δ_C ($CDCl_3$) 23.83 (CH_3), 27.71 (CH_3), 31.42 (CH_3), 61.15 (CH), 65.53 (C), 100.56 (CH), 126.04, 128.38, 128.44 (Ph), 135.48 (C), 148.17 (C), 152.15 (C), 162.10 (C). Anal. ($C_{14}H_{16}N_2O_3$) C, H, N. MS: m/e = 272 (M^+).

General Procedure for the Synthesis of Compounds 12a,b and 13−15. An Example: 3-Methyl-6-(2″-methyl-2″-oxiranylmethyl)-2′,3′,5′-tri-*O*-benzoyluridine (12a). To a solution of 3,6-dimethyl-2′,3′,5′-tri-*O*-benzoyluridine **11** in dry THF (6 mL) cooled to −78 °C, freshly prepared lithium diisopropylamide (LDA, 1.5 mmol) was added dropwise under a nitrogen atmosphere. After the mixture was stirred for 30 min, chloroacetone (1.3 mmol) was added while maintaining the temperature below −70 °C. The mixture was stirred for 6 h, quenched with a saturated NH_4Cl solution (1 mL), and allowed to warm to room temperature. The organic layer diluted with EtOAc (60 mL) was then separated, dried with Na_2SO_4, and evaporated under reduced pressure. The residue was purified by flash chromatography using $CHCl_3$/MeOH = 9.5:0.5 as the mobile-phase to give compounds **12a** in 80% yield (Table 1): oil, ν_{max} (cm^{-1}) 2988, 1720, 1680, 1540, 1420; δ_H ($CDCl_3$) 1.30 (3H, m, CH_3), 2.10 (2H, m, CH_2), 3.38 (3H, s, *N*-CH_3), 4.0−4.20 (2H, m, CH), 4.50−4.80 (3H, m, CH + CH_2), 5.61 (1H, s, CH), 6.15 (2H, m, CH), 6.64 (1H, m, CH), 7.30−8.10 (15H, m, Ph−H); δ_C ($CDCl_3$) 20.80 (CH_3), 27.78 (CH_3), 38.44 (CH_2), 48.39 (CH_2), 58.56 (C), 63.59 (CH_2), 70.75 (CH), 73.31 (CH), 81.0 (CH), 81.43 (CH), 98.46 (CH), 128.20 (CH), 128.71 (CH), 128.90 (CH), 129.42 (CH), 130.96 (C), 132.60 (CH), 132.92 (C), 135.59 (CH), 146.85 (C), 159.80 (C), 160.41 (C), 162.31 (C), 166.84 (C), 170.0. Anal. ($C_{35}H_{32}N_2O_{10}$) C, H, N. MS: m/e = 640 (M^+).

Biology. SV Growth Inhibition Assay in MDCK Cells. MDCK cells were grown in RPMI 1640 supplemented with 5% fetal calf serum (FCS) and antibiotics in a 5% CO_2 atmosphere. Confluent cell monolayers were infected with SV (10 HAU/10^5 cells) prepared by allantoic inoculation of embrionated eggs. After incubation for 1 h at 37 °C (adsorption period), virus inocula were removed, monolayers were washed three times with PBS and incubated with fresh medium containing 2% FCS. All the products were added, at the appropriate dilution, after the adsorption period and maintained in the culture media until the end of the experiments.

Molecular Modeling and Pharmacophore Generation Studies. A training set of 22 derivatives with biological data

ranging from 0.18 to 893 μM was selected from the original set and used in this study.

To find a pharmacophore able to describe the ligand−receptor interactions, instead of a superimposition approach based on atoms or groups of the chemical structures, the following steps have been carried out by means of the Catalyst software.

i. Energy Minimization, Geometry Optimization, and Conformational Analysis of all the Compounds of the Training Set. Because no experimental data on the biologically relevant conformations of these compounds are available (for example, atomic coordinates derived from X-ray crystallographic studies of the complexes between the receptor with an embedded inhibitor), there was a need to build their conformational models to be used in the hypothesis generation step. Moreover, it is well-known that the biological activity of chiral compounds is usually due to one of the diastereoisomers or enantiomers. Because of this fact and taking into account the presence of at least one asymmetric carbon atom common to all the compounds of the training set, it was arbitrarily decided to model the chiral compounds with undefined chirality, allowing the pharmacophore model generation procedure to choose which configuration of the asymmetric carbon atoms was the most appropriate. Compounds **5d** and **10a**−**c** were modeled with the appropriate *Z*,*E* stereochemistry and with undefined *R*,*S* chirality. The enantiomer or diastereoisomer of each compound chosen by the program to fit the proposed pharmacophore model has been reported in Table 1. To the best of our knowledge, there are no experimental data supporting the hypothesis that specific enantiomers or diastereoisomers are more active than the corresponding mirror-image enantiomers or diastereoisomers because of the fact that any enantiopure compound has been evaluated for its inhibitory properties against the Sendai virus.

The compounds used in this study were built using the Catalyst 2D-3D sketcher, and a representative family of conformations were generated for each molecule using the Poling algorithm[33] and the "best conformational analysis" method. This approach has been selected because it represents the method of choice when the conformations are to be used for hypothesis generation, as in this case.

Conformations were selected that fell within 20 kcal/mol range above the lowest energy conformation found.

ii. Generation of Binding Hypotheses for Compounds of the Training Set and Analysis of the Generated Hypotheses. The training set of molecules, with their associated conformational models, was submitted to hypothesis generation. The chemical functions used in this generation step included "hydrogen bond acceptor lipid" (HBA), "hydrophobic" (HY), and "ring aromatic" (RA).[34] The hydrogen bond acceptor lipid includes the basic nitrogen not considered in the hydrogen bond feature. A ring aromatic function was used in addition to the generic hydrophobic one in order to emphasize that an aromatic interaction is likely to be an important feature because some of the compounds present an aromatic ring within their structure. Moreover, the ring aromatic function allows consideration of directionality of the interactions with the receptor showing the ring centroid and a projected point along the normal to the ring plane.

Because of the small molecular size of compounds of the training set, the minimum permitted interfeature spacing was reduced to 1 Å. The default value of about 3 Å works well for most medium to large molecules, but it is not good for small molecules that do not have many features or for hypotheses where features are close together. In addition, the hypothesis generator was constrained to report only hypotheses with four features.

To be considered available, a chemical function must be surface accessible and thus able to interact with the receptor.[32] On the basis of these considerations, while the carbonyl and methoxy groups are classified as HBA by the program (see compounds **2b** and **5e**), oxygen atoms of substituents larger than methoxy groups are buried and thus unable to interact with the hypothetical receptor.

The ideal and null hypotheses have a cost of 90.76 and 163.01 bits, respectively, while the 10 resulting hypotheses possessed costs from 118.30 to 133.45 bits. Although the program assigns a general score to each hypothesis generated (based on the correlation between the observed and estimated activities for each compound in the training set), a thorough analysis of the structural and functional fitting of compounds listed in Table 1 was carried out in order to select the hypothesis that would represent better the most active compounds. We expected that the best hypothesis selected (hypothesis 1) corresponds to the most probable common arrangement of chemical functionalities for this set of Sendai virus inhibitors. The best hypothesis, which was confirmed by the Fischer test to have at least a 95% chance of true correlation, yielded a low rmsd of 1.40 and an *r* of 0.85, indicating a good correlation among the data in the training set.

The validity and predictive power of hypothesis 1 were further assessed using anti-SV compounds outside the training set. The predicted activities of such compounds, calculated by Catalyst on the basis of the pharmacophore model, are reported in Table 1.

Acknowledgment. Financial support from Italian MURST and Italian Ministry of Healt is acknowledged. Italian Research National Council of Italy (CNR Target Project on "Biotechnology") is also acknowledged. M. Botta expresses thanks for a grant from the Merck Research Laboratories (Academic Development Program in Chemistry).

Supporting Information Available: NMR and MS data. This material is available free of charge via the Internet at http://pubs.acs.org.

References

(1) Lamb R. A.; Kolakofsky D. Paramyxoviridae and Their Replication. In *Fields Virology*, 3rd ed.; Fields B. N., Knipe D. M., Howley, P. M., Eds.; Lippincott-Raven Publishers: Philadelphia, 1996; pp 1177−1194

(2) Morris, J. A.; Blount, R. E., Jr.; Savage, R. E. Recovery of Cytopathogenic Agent from Chimpanzees with Coryza. *Proc. Soc. Exp. Biol. Med.* **1956**, *192*, 544−549.

(3) Chanock, R. M. Association of a New Type of Cytopathogenic Myxovirus with Infantile Croup. *J. Exp. Med.* **1956**, *104*, 555−563.

(4) Chanock, R. M.; Parrott, R. H.; Cook, K. Newly Recognized Myxoviruses from Children with Respiratory Disease. *N. Engl. J. Med.* **1958**, *258*, 207−213.

(5) Welliver, R.; Wong, D. T.; Choi, T. S.; Ogra, P. L. Natural History of Parainfluenza Virus Infection in Childhood. *J. Pediatr.* **1982**, *101*, 180−187.

(6) Todd Faulks, J.; Drinka, P. J.; Shult, P. A Serious Outbreak of Parainfluenza Type 3 on a Nursing Unit. *J. Am. Geriatr. Soc.* **2000**, *48*, 1216−1218.

(7) Wendt, C. H.; Weisdorf, D. J.; Jordan, M. C.; Balfour, H. H., Jr.; Hertz, M. I. Parainfluenza Virus Respiratory Infection after Bone Marrow Transplantation. *N. Engl. J. Med.* **1992**, *326*, 921−926.

(8) Hohenthal, U.; Nikoskelainen, J.; Vainionpaa, R.; Peltonen, R.; Routamaa, M.; Itala, M.; Kotilainen, P. Parainfluenza Virus Type 3 Infections in a Hematology Unit. *Bone Marrow Transplant.* **2001**, *27*, 295−300.

(9) Gelfand, E. W.; McCurdy, D.; Rao, C. P.; Middleton, P. J. Ribavirin Treatment of Viral Pneumonitis in Severe Combined Immunodeficiency. *Lancet* **1983**, *2*, 732−733.

(10) McIntosh, K.; Kurachek, S. C.; Cairns, L. M.; Burns, J. C.; Goodspeed, B. Treatment of Respiratory Viral Infection in an Immunodeficient Infant with Ribavirin Aerosol. *Am. J. Dis. Child.* **1984**, *138*, 305−308.

(11) Elizaga, J.; Olavarria, E.; Apperley, J.; Goldman, J.; Ward, K. Parainfluenza Virus 3 Infection after Stem Cell Transplant: Relevance to Outcome of Rapid Diagnosis and Ribavirin Treatment. *Clin. Infect. Dis.* **2001**, *32*, 413−418.

(12) Canonico, P. G.; Kende, M.; Huggins, J. W. Toxicology and Pharmacology of Ribavirin in Experimental Animals. In *Clinical Applications of Ribavirin*; Smith R. A., Knight V., Smith J. A. D., Eds.; Academic Press: Orlando, FL, 1984; pp 65−98.

(13) (a) Ishida, N.; Homma, M. Sendai Virus. *Adv. Virus Res.* **1978**, *23*, 349−383. (b) Amici, C.; Palamara, A. T.; Garaci, E.; Santoro, M. G. Inhibition of Sendai Virus Replication by Δ12-Prostaglandin J2: Induction of Heat Shock Protein Synthesis and Alteration of Protein Glycosylation. *Antiviral Res.* **1992**, *19*, 129−138.

(14) Ono, A.; Kawakita, M. Transport of Envelope Proteins of Sendai Virus, HN and FO, Is Blocked at Different Steps by Thapsigargin and Other Perturbants to Intracellular Ca^{2+}. *J. Biochem. (Tokyo)* **1994**, *116*, 649−656.

(15) Iliescu, R.; Calinoiu, A.; Repanovici, R.; Popa, L. M.; Loeber, G. Effect of Ambazone on the Multiplication and Biological Activities of Sendai Virus. *Stud. Biophys.* **1987**, *117*, 111−116.

(16) Iida, J.; Ishihara, C.; Mizukoshi, N.; Kitoh, K.; Tsukidate, K.; Katsu, K.; Toyosawa, T.; Azuma, I. Prophylactic Activity of Dihydroheptaprenol, a Synthetic Polyprenol Derivative, against Sendai Virus Infection in Mice. *Vaccine* **1990**, *8*, 376−380.

(17) Kimsey, P. B.; Goad, M. E.; Zhao, Z. B.; Brackee, G.; Fox, J. G. Methyl Prednisolone Acetate Modulation of Infection and Subsequent Pulmonary Pathology in Hamsters Exposed to Parainfluenza-1 Virus (Sendai). *Am. Rev. Respir. Dis.* **1989**, *140*, 1704−1711.

(18) Saladino, R.; Danti, M. C.; Mincione, E.; Crestini, C.; Palamara, A. T.; Savini, P.; Marini, S.; Botta, M. A Potent and Selective Inhibition of Parainfluenza 1 (Sendai) Virus by New 6-Oxiranyl-, 6-Methyloxiranyluracils, and 4(3*H*)-Pyrimidinone Derivatives. *Bioorg. Med. Chem. Lett.* **1998**, *8*, 1833−1838.

(19) Catalyst 4.5 is from MSI Software, Scranton Road, MA.

(20) (a) Tanaka, H.; Takashima, H.; Ubasawa, M.; Sekiya, K.; Nitta, I.; Baba, M.; Shigeta, C. S.; Walzer, R. T.; De Clercq, E.; Miyasaka, T. Synthesis and Antiviral Activity of Deoxy Analogs of 1-[(2-Hydroxyethoxy)methyl]-6-(phenylthio)thymine (HEPT) as Potent and Selective Anti-HIV-1 Agents. *J. Med. Chem.* **1992**, *35*, 4713−4719 and references therein. (b) Artico, M.; Massa, S.; Mai, A.; Marongiu, M. E.; Piras, G.; Tramontano, E.; La Colla, P. 3,4-Dihydro-2-alkoxy-6-benzyl-4-oxopyrimidines (DABOs): A New Class of Specific Inhibitors of Human Immunodeficiency Virus Type 1. *Antiviral Chem. Chemother.* **1993**, *4*, 361−368.

(21) Tanaka, H.; Baba, M.; Hayakawa, H.; Sakamaki, T.; Miyasaka, T.; Ubasawa, M.; Takashima, H.; Sekiya, K.; Shigeta, S.; Walzer, R. Y.; Balzarini, J.; De Clercq, E. A New Class of HIV-1 Specific 6-Substituted Acyclouridine Derivatives: Synthesis and Anti-HIV-1 Activity of 5- or 6-Substituted Analogues of 1-[(2-Hydroxyethoxy)methyl]-6-(phenylthio)thymine (HEPT). *J. Med. Chem.* **1991**, *34*, 349−357.

(22) Botta, M.; Saladino, R.; Gambacorta, A.; Nicoletti, R. An Unusual Condensation of Pyrimidinones: Synthesis of Bipyrimidinones and Bipyrimidinylmethane. *Heterocycles* **1991**, *32*, 1537−1545.

(23) Botta, M.; Saladino, R.; Delle Monache, G.; Gentile, G.; Nicoletti, R. Research on Antiviral Agents. 5. Lithiation of 6-Methyluracil as a New and Efficient Entry to C(6)-Substituted Uracils. *Heterocycles* **1996**, *43*, 1687−1696.

(24) 4-Chlorobutyraldeide was obtained by oxidation of 4-chloro-1-butanol with pyridinium chlorocromate (PCC) in CH_2Cl_2 at 25 °C.

(25) Botta, M.; De Angelis, F.; Finizia, G.; Gambacorta, A.; Nicoletti, R. 6-Alkyl- and 5,6-Dialkyl-2-methoxy-4(3*H*)-pyrimidinones in the Transformation of Pyrimidines. Conversion into 2-Substituted Amino- and 4-Chloro-pyrimidine Derivatives. *Synth. Commun.* **1985**, *15*, 27−34.

(26) Compound **11** was prepared in a regiospecific manner starting from commercially available 1-*O*-acetyl-2,3,5-tri-*O*-benzoyl-*β*-D-ribofuranose and 2,4-dihydroxy-6-methylpyrimidine as described in ref 35 followed by subsequent N-3 methylation with CH_2N_2 in MeOH at 25 °C.

(27) Botta, M.; Saladino, R.; Occhionero, F.; Nicoletti, R. Recent Advances in the Chemistry of 6-Substituted Pyrimidines and Uracil Derivatives. *Trends Org. Chem.* **1995**, *5*, 57−81.

(28) Garaci, E.; Palamara, A. T.; Di Francesco, P.; Favalli, C.; Ciriolo, M. R.; Rotilio, G. Glutathione Inhibits Replication and Expression of Viral Proteins and Cultured Cells Infected with Sendai Virus. *Biochem. Biophys. Res. Commun.* **1992**, *188*, 1090−1096.

(29) ED_{50}, MTC, and CC_{50} values for compounds **12**−**15** (expressed as μM concentrations) are reported below. **12a**: 97, 156, 220. **12b**: >142, 142, 369. **13**: 151, 151, 386. **14**: 90, 151, 432. **15**: 77, 136, 313.

(30) The rules for picking training sets are reported at http://www.msi.com/support/catalyst/hypogen.html.

(31) Fischer, R. The Principle of Experimentation, Illustrated by a Psycho-Physical Experiment. In *The Design of Experiments*; Hafner Publishing Co.: New York, 1966; Chapter II.

(32) For example, a hydrogen bond acceptor, such as a carbonyl group or an alkoxy group, is not perceived unless the environment around the group itself is sufficiently uncrowded.

(33) Smellie, A.; Teig, S.; Towbin, P. Poling: Promoting Conformational Coverage. *J. Comput. Chem.* **1995**, *16*, 171−187.

(34) Greene, J.; Kahn, S.; Savoj, H.; Sprague, P.; Teig, S. Chemical Function Queries for 3D Database Search. *J. Chem. Inf. Comput. Sci.* **1994**, *34*, 1297−1308.

(35) Botta, M.; De Angelis, F.; Finizia, G.; Nicoletti, R.; Delfini, M. 6-Alkyl- and 5,6-Dialkyl-2-methoxy-4(3*H*)-pyrimidinones in the Transformations of Pyrimidines. Regiospecific 1-*N*-Acylation of Pyrimidines. *Tetrahedron Lett.* **1985**, *26*, 3345−3348 and references therein.

JM010938I